

1 Article

2 Study of the Mobilization of Uranium Isotopes in a 3 Sandstone Aquifer Using Methods for the Extraction 4 of Uranium with Different Strength Reagents in 5 Combination with Groundwater Data

6 Alexander I. Malov* and Sergey B. Zykov

7 Federal Center for Integrated Arctic Research of Russian Academy of Sciences; Arkhangelsk, 163061, Russia;
8 malovai@yandex.ru; abs2417@yandex.ru

9 * Correspondence: malovai@yandex.ru; Tel.: +7-911-571-71-72

10

11 **Abstract:** A partial extraction procedure was used to study the distribution of uranium in the
12 mineral phases of rocks of an aquifer of sandy-clay deposits of the Vendian in the northwest of
13 Russia. This work is a part of a research project to develop a method for combined radiocarbon and
14 uranium-isotope dating of groundwater. Representative aliquots of each core sample were
15 subjected to five "partial" extractions by treatment with: distilled water, low mineralized fresh
16 natural groundwater, minopolycarboxylic acid chelating agent (0.05M EDTA), 0.5M HCl, 15M
17 HNO₃, and a total digestion, with U isotopes reported in this study for each procedure. The
18 following mineral phases of core samples: adsorbed material, carbonate minerals, amorphous iron
19 oxides, aluminosilicates partial digestion and a crystalline iron oxides, aluminosilicates total
20 digestion and a clay/quartz resistate were characterized. Red-colored siltstones depleted in
21 uranium in relatively readily soluble mineral phases. The concentration of adsorbed uranium was
22 established in the amount of 15.8±2.1 - 30.5±3.9 µg/kg. Carbonate minerals contain even less of this
23 element. In iron hydroxides and the most readily soluble aluminosilicates, its concentrations are in
24 the range 168±24 - 212±28 µg/kg. The most insoluble fraction contains 1.65±0.21 - 4.32±0.45 mg/kg of
25 uranium. In green-colored siltstones, the concentration of adsorbed uranium is much higher:
26 106±14 - 364±43 µg/kg. Carbonate minerals and amorphous iron oxides contain 1.91±0.21 - 2.34±0.26
27 mg/kg of uranium. In aluminosilicates and a clay/quartz resistate, uranium concentrations are
28 5.6±0.5 - 16.8±1.4 mg/kg. Elevated values of ²³⁴U:²³⁸U activity ratio prevail in the adsorbed material
29 and iron hydroxides. In aluminosilicates and clay/quartz resistate, the values decrease. This
30 indicates the replacement of primary sedimentogenic uranium by secondary hydrogenic uranium
31 adsorbed on the surface of minerals and coprecipitated with iron hydroxides. The results obtained
32 made it possible to carry out preliminary quantitative estimates of the retardation factor and recoil
33 loss factor of uranium in the groundwater of siltstones of the studied Vendian aquifer.

34 **Keywords:** Partial extraction, Mineral phases, Uranium, Disequilibrium, Retardation factor

35 1. Introduction

36 Uranium isotopes are a powerful tool for refining conceptual models of groundwater [1–4],
37 groundwater dating [5–7] and descriptions of chemical weathering processes [8–10] for up to
38 hundreds of thousands of years [11]. The main initial parameters are i) measured concentration of
39 ²³⁸U in the combined solution and solid phase, and ii) measured ²³⁴U:²³⁸U activity ratio in the

40 combined pore fluid and solid phase. They can be obtained by direct measurements in water and
41 rock samples taken in the field.

42 However, the interpretation of the results is rather complicated. This is due to the heterogeneity
43 of the rocks in their composition. For example, sandy clay sediments of aquifers can contain both
44 poorly soluble grains of quartz and feldspar, as well as soluble carbonate and gypsum cements.
45 Carbonates, iron oxides, and clay minerals are characterized by increased U adsorption on their
46 surfaces [12–14]. Further, daughter nuclides pass most actively into water from surface coatings [15],
47 increasing the ratio of isotope activities in water. In addition, the similarity of the activity ratios of
48 $^{234}\text{U}:$ ^{238}U in groundwater and in the most easily leached fractions of water-bearing rocks was noted in
49 the experiments of Lawson et al. [16], Payne et al. [17], and Dabous et al. [18]. These fractions were
50 defined as adsorbed elements, carbonate minerals and amorphous iron minerals [19]. This may
51 indicate the opposite process: the transition of nonequilibrium nuclides from water to rock with an
52 increase in the ratio of U isotope activities in the rock [20]. Under such conditions, it is difficult to
53 estimate the rate of chemical weathering by using the currently developed methods [21–22].

54 Therefore, for a more complete understanding of the behavior of uranium isotopes in the
55 water-rock system, a transition from the presentation of solely total concentration and activity data
56 to an additional analysis for finding individual “weak” leach extractants or sequential extractions is
57 necessary. In recent decades, leach data, rather than total decomposition data are widely used in a
58 variety of fields of geocology (see for example [23–26]). Therefore, in the present work, an attempt is
59 made to use the partial extraction procedure for reconstructing the processes of redistribution of
60 uranium isotopes in certain mineral phases of an aquifer of sandy-clay deposits of the Vendian.

61 In a previous papers [27–28], the possibility of sharing uranium and carbon isotopes for dating
62 groundwater was discussed. The transport of uranium in solution is reasonably well described with
63 a standard advection-dispersion-exchange formulation:

64 $\Delta t_{\text{time}} = \text{advection} + \text{weathering} + \text{recoil} + \text{desorption} + \text{production} - \text{precipitation} - \text{decay} - \text{adsorption}$
65 [5–7]. Among the many factors, the main ones are t – Groundwater residence time in the aquifer
66 (time), v – Groundwater flow velocity (advection), R_d – Dissolution rate (weathering - precipitation),
67 R – Retardation factor (adsorption - desorption), p – Recoil loss factor (recoil + production), and λ_4 –
68 Decay constants for ^{234}U (decay). Suitable equations were derived by Andrews and Kay [29],
69 Fröhlich and Gellermann [30], Ivanovich et al. [9], and Porcelli [5] to provide a ^{234}U – ^{238}U dating
70 method for groundwater under oxidizing conditions. However, the values of R , R_d (a^{-1}) and p needed
71 to be determined. In turn, the recoil loss factor value p depends on the SSA (specific surface area).
72 The published SSA values in sandy aquifers range from 0.9–1.8 $\text{m}^2\cdot\text{kg}^{-1}$ [31] to 330–390 $\text{m}^2\cdot\text{kg}^{-1}$ [6].
73 Accordingly, the ranges of R and R_d can be calculated using these formulas. Therefore, we consider it
74 more appropriate to show R , R_d and p in the form of their ratios: $R_d:p$ (a^{-1}), $R:p$ and $R_d:R$ (a^{-1}). The
75 main calculated equations are as follows [27]:

$$76 \quad t = \frac{\ln(k^{-1})}{\lambda_4}, \text{ where } k = 1 - \frac{C_8^W \cdot R \cdot (AR_t - 1)}{M_s \cdot C_8^R \cdot p} \quad (1)$$

77 Where C_8^W is the concentration of uranium in water; C_8^R is the concentration of uranium in
78 the rock; AR_t - $^{234}\text{U}/^{238}\text{U}$ is the activity ratio in the water sample; M_s is the solid mass to fluid
79 volume ratio.

80 In this case, two unknown parameters remain in formula (1), which cannot be directly
81 measured in water and rock samples: t and R/p . Therefore, in order to use equation (1), it is
82 necessary to make several determinations of the groundwater age by other methods, for example,
83 using isotopes of carbon. Then, we need to find out whether there is an increase in uranium
84 concentrations in groundwater with a decrease in the concentration of radiocarbon. If this is the case,
85 then the mean values R/p for the studied aquifers are determined. After this, uranium-isotopic
86 dating of other groundwater samples is carried out, which is less labor-intensive and more accessible
87 than radiocarbon dating. The average value of the retardation factor/recoil loss factor ratio (R/p) in
88 samples from the sandstone aquifer of the upper Vendian strata and overlying horizons is assumed
89 to be (24±4) [27].

90 In this work, it was planned, by determining the amount of uranium adsorbed on the surface of
91 mineral particles, to proceed to a separate assessment of the values of the retardation factor and
92 recoil loss factor of uranium in the groundwater of siltstones of the studied Vendian aquifer.

93 2. Materials

94 The borehole GGS2-11 is located in the northwest of Russia at the diamond deposit area
95 (N65°20'48" E41°06'10") and was drilled using a diamond drill bit (92 mm inner diameter, 112 mm
96 outer diameter) and mud rotary methods to 101.2 m below ground surface in July 2018. This core
97 was selected for the present study because the sampled section traverses the aquifer of the Padun
98 formation of the Vendian (Vpd) [27, 28] which is of interest in the present study. For this study, 5
99 samples were taken from the intervals of 66.7-66.8, 75.2-75.3, 83.9-84, 94-94.1, 99.5-99.6 m (Fig. 1).

100 The samples were quickly packed in airtight polythene bags. The sample mass collected in each
101 case was about 1500 g. Sub-samples of the material were oven dried at 40 °C for 7 days and
102 homogenized by grinding with an agate mortar and pestle to pass through a 125 μm sieve. The
103 prepared material was stored in glass bottles for sequential extractions and isotopic analyses.

104 The chemical and mineralogical composition of the Vendian deposits in the area of the diamond
105 deposit was studied in detail during different periods of geological exploration [32-35]. The Padun
106 Formation, 160 m thick, mainly consists of sandstones (60-80%) and siltstones (20-30%) separated by
107 mudstone interlayers. The rocks have reddish brown color with pale green lenses and patches. The
108 sandstones are dominated by fine- and medium-grained varieties. The content of pelitic particles
109 does not exceed 20%. Clastic material is represented by quartz. Feldspars, chalcedony, quartzite
110 fragments, biotite, and clayey aggregates are insignificant. The cement has mainly a clayey
111 (hydromicaceous)-ferruginous composition. Carbonate and gypsum cement is also encountered. In
112 the upper part of the sequence (thickness ~50 m), the sandstones are poorly cemented and often
113 represented by sands. The siltstones are dominated by the coarse-grained fraction. The clastic grains
114 consist of quartz (up to 98%), feldspars (up to 10%), and micas (~1%). The cement has
115 clayey-ferruginous, carbonate-clayey, and less common gypsum compositions. Clay minerals are
116 observed as hydromicas, kaolinite, and chlorite. Bitumen and organic carbon are nearly absent. The

117 ratio of Fe_2O_3 and FeO forms of iron in "red" siltstones is ~ 17: 1. In "green" siltstones, the Fe_2O_3
 118 content is 2.7 times lower (Table 1).
 119



120

121 **Figure 1.** Photos of samples of studied rocks. 1 - Green siltstones, 66.7-66.8 m. 2 - Red sandstones,
 122 75.2-75.3 m. 3 - Variegated siltstones, 83.9-84 m. 4 - Red siltstones, 94-94.1 m. 5-6 - Green siltstones,
 123 99.5-99.6 m (photo S. Druzhinin)

124 The description of the samples of the studied rocks was performed on five thin sections of core
 125 samples (see Appendix A).

126 **Table 1.** The average chemical composition of the red siltstones of the Padun Formation of the
 127 Vendian in research area (from 18 determinations) [34] and green siltstones of the sample GGS2-11
 128 (depth 99.5 m), %

| | SiO_2 | Al_2O_3 | CaO | MgO | Na_2O | K_2O |
|------------------|----------------|-------------------------|--------------|--------------|-----------------------|----------------------|
| ^a RSi | 72 | 12.8 | 0.48 | 1.24 | 0.14 | 2.94 |
| ^b GSi | 74.6 | 12.5 | 0.39 | 1.34 | 0.16 | 4.48 |

| | Fe_2O_3 | FeO | TiO_2 | Cr_2O_3 | MnO | P_2O_5 | ^c LOI |
|------------------|-------------------------|--------------|----------------|-------------------------|--------------|------------------------|------------------|
| ^a RSi | 5.3 | 0.3 | 0.81 | 0.02 | 0.14 | 0.07 | 3.36 |
| ^b GSi | 1.99 | 0.3 | 0.91 | 0.07 | 0.01 | 0.11 | 2.74 |

129

130 ^aRSi - red siltstones. ^bGSi - green siltstones. ^cLOI - loss on ignition.

131 3. Methods

132 Representative aliquots of each core sample were subjected to five "partial" extractions and a
 133 total digestion, with U isotopes reported in this study for each procedure. The various procedures
 134 are described hereinafter.

135 3.1. Partial extractions

136 *Distilled water*

137 500 ml distilled water was mixed with 50 g of core sample in centrifuge tubes and shaken for 1
138 hr on an end-over-end shaker at room temperature. The short duration of the laboratory
139 experiments suggests that dissolution depends upon the ease with which the fine particulates may
140 be freed from the rock surface [36-37]. Firstly, this procedure refers to adsorbed particles.

141 *Low mineralized fresh natural groundwater*

142 500 ml of low mineralized water of Ca-Mg-Na-HCO₃ composition from the borehole had total
143 dissolved solids (TDS) of 285 mg/L (see [28]) and was mixed with 50 g of core sample in centrifuge
144 tubes and shaken for 1 hr on an end-over-end shaker at room temperature. Firstly, adsorbed
145 material was released.

146 The following four stages were carried out according to the method proposed by Sutherland et
147 al. [26].

148 *0.05M EDTA*

149 Aminopolycarboxylic acid chelating agent (EDTA) at the concentration and pH level used in
150 this study was the weakest extractant after fresh groundwater [26]. As an extractant, EDTA has
151 been widely used in environmental geochemistry. Complexants like EDTA are frequently used to
152 release the readily available (labile) fraction of materials [26]. In our case, this is carbonate cement.
153 The procedure outlined by Singh et al. [38] was followed in this study. 500 mL of 0.05M EDTA (pH
154 7) was mixed with 50 g of core sample in centrifuge tubes and shaken for 1 hr on an end-over-end
155 shaker at room temperature.

156 *0.5M HCl*

157 According to a review by Sutherland et al. [26], HCl dissolves complexed, adsorbed,
158 precipitated, amorphous or poorly crystallized Fe compounds without significant attack on the
159 crystal lattice. In the present study, 500 mL of 0.5M HCl was mixed with 50 g of core sample and
160 shaken at room temperature for 1 hr on an end-over-end shaker.

161 *15M HNO₃*

162 Nitric acid is an oxidizing agent that is not as powerful in its attack on aluminosilicates as HF,
163 and is thus said to be a partial digestion. Also, crystalline iron oxide is digested by hot HNO₃. In the
164 present study, 500 mL of 15M HNO₃ was mixed with 25 g of core sample and heated for 1 hr while
165 stirring. The resulting solution was evaporated to wet salts, topped up with 500 ml of distilled water
166 and acidified with HCl to pH 1-2.

167 3.2. Measurements of uranium isotopes after five "partial" extractions

168 Determinations of uranium isotopes in the resulting solution were made in accordance with
169 Malyshev et al. [39] which is also described in Fröhlich [40]. Spectrometric detection of alpha
170 particles was performed using an alpha spectrometer (PROGRESS-ALPHA, 'DOZE', Russia) with
171 uncertainty of 10-15%. Total error of analysis is defined by $\delta = \delta_{st} + \delta_{sys}$ (statistical + systematic).
172 Measurement uncertainties for U are reported individually (Table 2). Efficiency of ²³²U extraction
173 was 40-50%.

174 3.3. Total digestion

175 Measurements of uranium isotopes were made in accordance with Malyshev et al. [41]. For
176 these analyses, 10 g of core sample was placed in a porcelain crucible and calcined at 500 °C until
177 complete combustion of organic substances. The residue was transferred into a Teflon cup wetted
178 with distilled water. A weighed amount of spiked solution (with known activity of internal
179 standard ²³²U) was added, followed by 10 cm³ of 15M HNO₃ and then heated until the reddish
180 brown NO₂ gas vapor disappears. Then after cooling 40 cm³ of 29M HF and 10 cm³ of 12M HClO₄
181 were added. The covered Teflon cup was heated until HClO₄ vapor appeared. HF treatment was
182 repeated twice; the cup was cooled each time before adding acid and heating until HClO₄ fumes
183 were visible. After dissolution and cooling, the edge of the cup and the cover were rinsed with
184 distilled water and the content was transferred to an open Teflon™ dish, where the solution was
185 evaporated again until dense white fumes appeared. This procedure was repeated twice. Finally,
186 the residue was evaporated to give moist salts, which were dissolved in boiling 7M HNO₃ (50 cm³).
187 The undissolved residue was filtered off and washed three times with 5-10 cm³ portions of hot 7M
188 HNO₃ and added to the solution. The U solution was transferred to a separatory funnel and a 30%

189 solution of freshly purified tributylphosphate in toluene was added to give an aqueous to organic
 190 phase ratio of 4:1. Radionuclides were extracted for 5 min. After phase separation, the lower layer
 191 was poured back into the beaker. The organic extract was washed twice with an equal volume of
 192 7M HNO₃, then with an equal volume of 0.25M HNO₃ solution in 0.04M HF. The back-extraction of
 193 uranium isotopes was performed by washing the organic phase with an equal volume of distilled
 194 water three times for 1 min each. The pooled aqueous extracts were evaporated to dryness, treated
 195 with 5 cm³ of concentrated HNO₃ to remove trace organic substances, and evaporated to dryness.
 196 The dry residue containing uranium was dissolved in 10 mL of 2% sodium carbonate with heating,
 197 then filtered. Dissolved uranium was electrodeposited on polished stainless steel plates for alpha
 198 spectrometry.

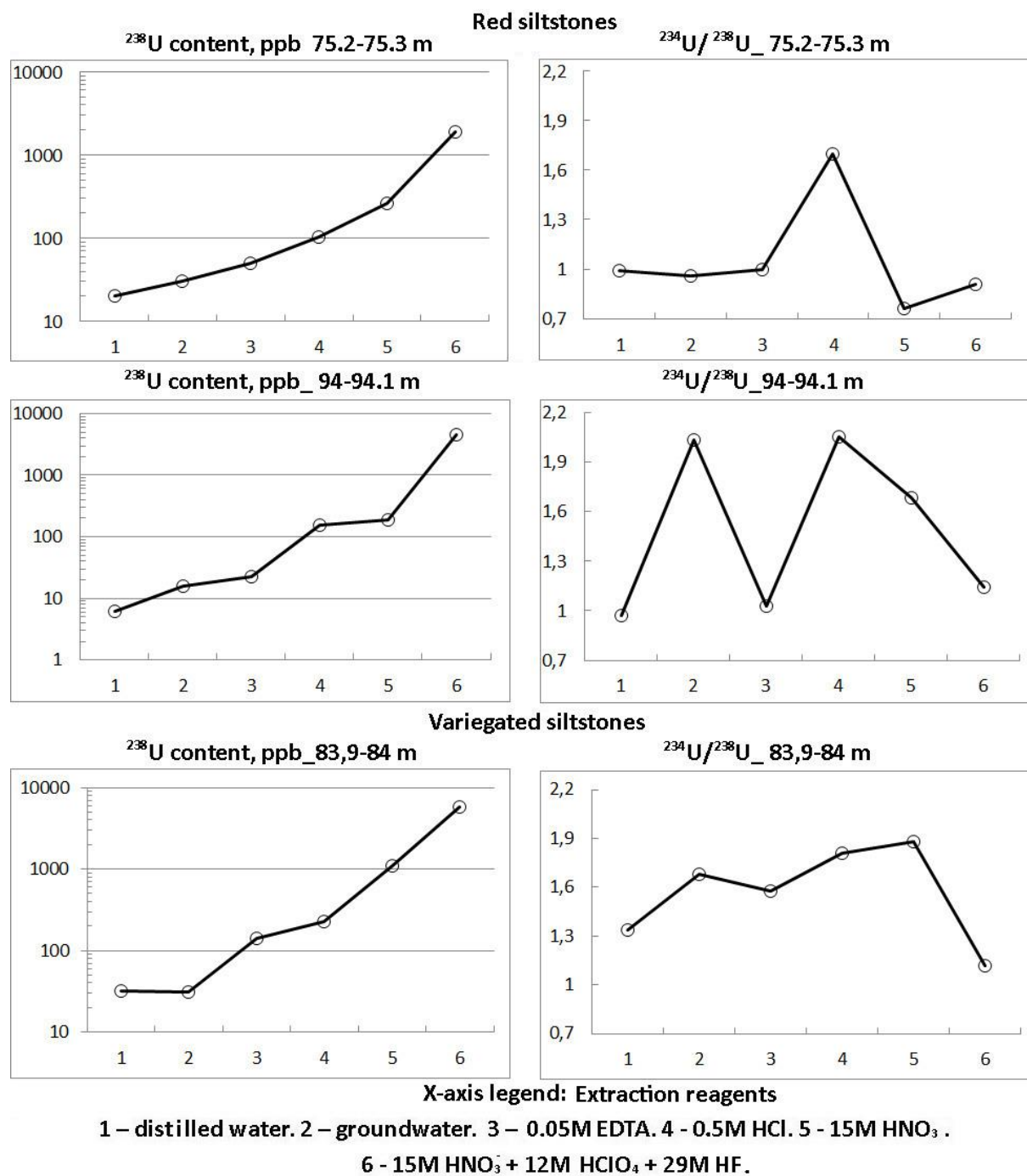
200 4. Results

201 Table 2 and Figs. 2 and 3 show the results of five “partial” extractions and total digestion of the
 202 five core samples.

203 **Table 2.** Distribution of uranium and measured ²³⁴U:²³⁸U activity ratios in extracted phases

| Solvent | ^a DW | ^b GW | 0.05M EDTA | 0.5M HCl | 15M HNO ₃ | 15M HNO ₃ + 12M HClO ₄ + 29M HF |
|---|-----------------|-----------------|-------------|-------------|----------------------|---|
| Substance dissolution, % | | | | | | |
| Red siltstones | 0.49 – 0.6 | 0.62 - 1 | 2.4 – 3.4 | 1.58 - 2.27 | 1.82 - 3.42 | 100 |
| Variegated siltstones | 1.04 | 0.82 | 1.88 | 2.3 | 4.34 | 100 |
| Green siltstones | 0.93 - 1.38 | 0.64 - 1.93 | 0.94 - 3.08 | 2.56 - 6.34 | 6.85 – 15.4 | 100 |
| Average | 0.89 | 1 | 2.34 | 3.01 | 6.37 | 100 |
| U content, µg/kg | | | | | | |
| Red siltstones 1 | 6.2±0.9 | 15.8±2.1 | 22.8±3.2 | 156±23 | 191±27 | 4510±467 |
| Red siltstones 2 | 20±2.6 | 30.5±3.9 | 50.3±7.4 | 103±14 | 262±34 | 1910±243 |
| Variegated siltstones | 31.6±4.6 | 30.9±4.1 | 140±19 | 230±28 | 1102±143 | 5840±578 |
| Green siltstones 1 | 80±11.1 | 106±14 | 857±102 | 2014±215 | 5086±512 | 18800±1504 |
| Green siltstones 2 | 95.3±11.4 | 364±43 | 1860±203 | 2708±302 | 3957±415 | 8328±707 |
| Average | 46.6 | 109 | 586 | 1042 | 2120 | 7878 |
| U content, % | | | | | | |
| Red siltstones | 0.14 - 1.1 | 0.35 - 1.6 | 0.51 - 2.6 | 3.5 - 5.4 | 4.2 - 13.7 | 100 |
| Variegated siltstones | 0.54 | 0.53 | 2.4 | 3.94 | 18.9 | 100 |
| Green siltstones | 0.43 - 1.14 | 0.56 - 4.37 | 4.56 - 22.3 | 10.7 - 32.5 | 27.1 - 47.5 | 100 |
| Average | 0.67 | 1.48 | 6.47 | 11.2 | 22.3 | 100 |
| ²³⁴U:²³⁸U activity ratio | | | | | | |
| Red siltstones | 0.97±0.14 | 0.96±0.13 | 1±0.14 | 1.7±0.25 | 0.76±0.11 | 0.91±0.13 |
| | 0.99±0.14 | 2.3±0.32 | 1.03±0.14 | 2.05±0.29 | 1.68±0.22 | 1.14±0.16 |
| Variegated siltstones | 1.34±0.19 | 1.68±0.23 | 1.58±0.21 | 1.81± 0.24 | 1.88±0.24 | 1.12±0.14 |
| Green siltstones | 1.87±0.26 | 1.65±0.2 | 1.39±0.2 | 1.03±0.15 | 0.98±0.14 | 1.12±0.14 |
| | 2.71±0.36 | 1.78±0.24 | 1.71±0.24 | 2.32±0.33 | 1.85±0.25 | 1.79±0.24 |
| Average | 1.58 | 1.67 | 1.34 | 1.78 | 1.43 | 1.22 |

204 ^aDW - Distilled water. ^bGW – groundwater.



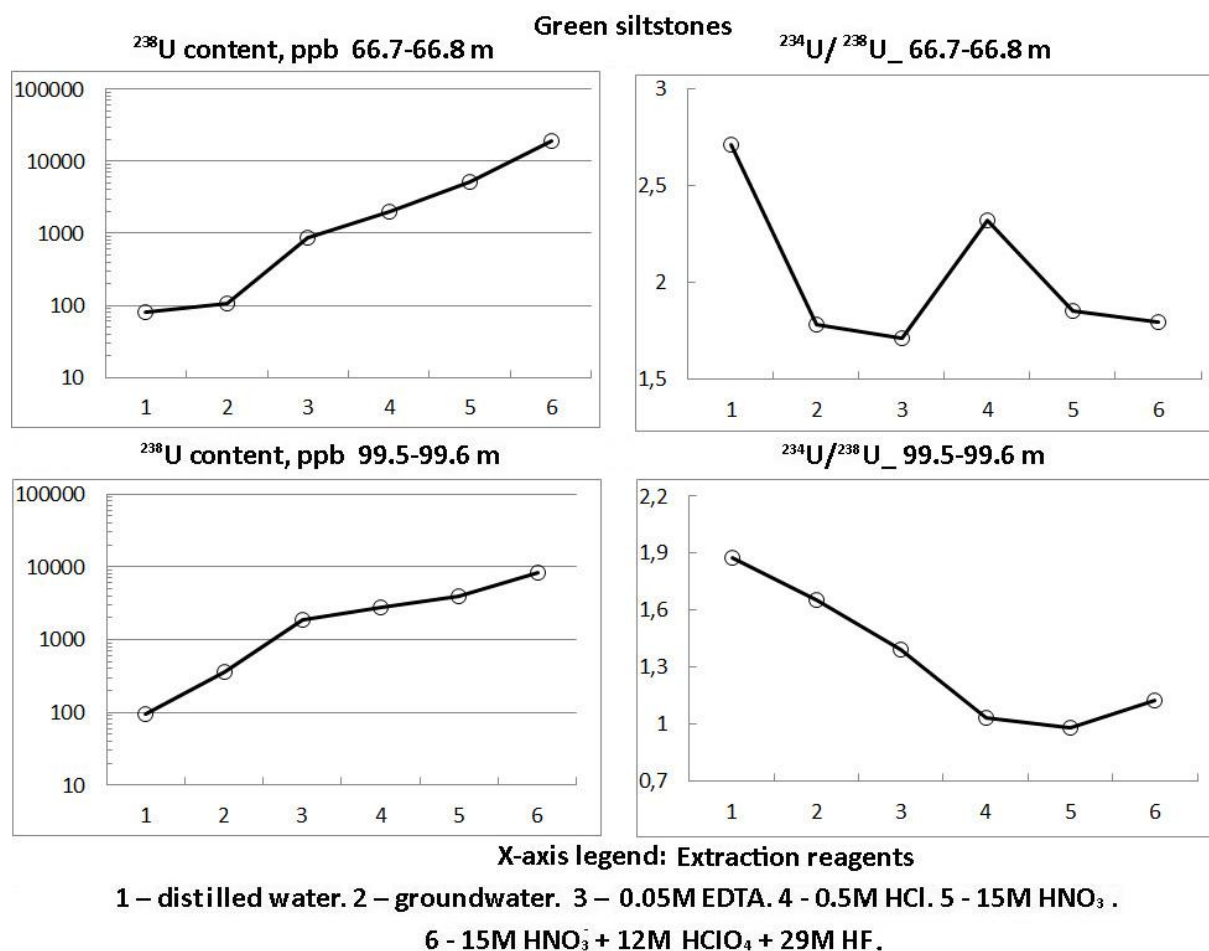
205

206

207

Figure 2. Distribution of ^{238}U content and $^{234}\text{U}/^{238}\text{U}$ activity ratio in phases 1-6, leached from crushed red and variegated siltstone of Vendian (Ediacaran) Padun Formations

208



209

210

211

Figure 3. Distribution of ^{238}U content and $^{234}\text{U}/^{238}\text{U}$ activity ratio in phases 1-6, leached from crushed green siltstone of Vendian (Ediacaran) Padun Formations

212

Substance dissolution

213

214

215

216

217

218

219

220

221

Uranium concentration

222

223

224

225

226

227

228

229

230

231

232

$^{234}\text{U}/^{238}\text{U}$ activity ratio

233

234

In red siltstones, the maximum values of $^{234}\text{U}/^{238}\text{U}$ activity ratio ($1.7\pm 0.25 - 2.3\pm 0.32$) were noted in the material dissolved in groundwater and 0.5M HCl. Minimum values ($0.76\pm 0.11 - 0.91\pm 0.13$) are

235 characteristic of the most difficultly soluble 15M HNO₃ and 15M HNO₃ + 12M HClO₄ + 29M HF
236 fractions of the studied rocks. In other cases, the values are close to unity.

237 In green siltstones, one increased value of ²³⁴U:²³⁸U activity ratio (2.32±0.33) was noted in a
238 material dissolved in 0.5M HCl. Three values close to unity were obtained by dissolving 0.5M HCl,
239 15M HNO₃ and 15M HNO₃ + 12M HClO₄ + 29M HF. However, in the remaining eight experiments,
240 using groundwater, 0.05M EDTA, 15M HNO₃, and 15M HNO₃ + 12M HClO₄ + 29M HF as a solvent,
241 the values of ²³⁴U:²³⁸U activity ratio were high: 1.39±0.2 – 2.71±0.36.

242 5. Discussion

243 *Substance dissolution*

244 In general, the percentage values of the substance dissolved under the influence of various solvents are
245 approximately consistent with the average chemical composition of siltstones of the Padun Formation of the
246 Vendian in the study area. EDTA, the weakest extractant after fresh groundwater, dissolved up to 3.4% of the
247 substance (Table 2). This corresponds to a loss on ignition (LOI) of 2.74 - 3.36% (Table 1), i.e. the carbonate
248 material of the cement of the studied rocks and other labile fractions. 0.5M HCl additionally dissolved up to 3%
249 of the substance, which is consistent with the content of Fe₂O₃ (2 - 5.3%) in Table 1, that is, it corresponds to
250 amorphous iron oxides. 15M HNO₃ additionally dissolved up to 9% of a substance that can only be represented
251 by the most readily soluble aluminosilicates. A mixture of 15M HNO₃ + 12M HClO₄ + 29M HF acids dissolves
252 the remainder of the aluminosilicates and a clay/quartz resistate.

253 *Uranium concentration*

254 Table 3 shows the uranium concentrations converted to mineral phases in µg/kg and %. In red siltstones,
255 the concentrations of adsorbed uranium were established in the amount of 15.8±2.1 - 30.5±3.9 µg/kg. This
256 amounts to 0.35 - 1.6% of its total amount in rocks of this type. Carbonate minerals contain even less uranium:
257 7±1 – 19.8±2.5 µg/kg. In iron hydroxides and the most readily soluble aluminosilicates, uranium concentrations
258 are in the range 52.7±7.2 - 133±19 and 35±5 - 159±21 µg/kg, respectively. This amounts to a total of 3.7 - 11.1%
259 of its total concentration. The most insoluble fraction contains 1.6±0.2 – 4.3±0.4 mg/kg of uranium. In green
260 siltstones, the concentration of adsorbed uranium is much higher: 106±14 - 364±43 µg/kg (0.56 - 4.37%). The
261 carbonate minerals and amorphous iron oxides contain a total of 1.91±0.21 – 2.34±0.26 mg/kg of uranium
262 (10.15 – 28.2%). In aluminosilicates and a clay/quartz resistate, the concentration of uranium amounts to
263 5.6±0.5 – 16.8±1.4 mg/kg.

264 **Table 3.** Distribution of uranium in the mineral phases.

| Defined phases of core samples | Adsorbed elements | Carbonate minerals | Amorphous iron oxides | Aluminosilicates partial digestion and a crystalline iron oxides | Aluminosilicates total digestion and a clay/quartz resistate |
|--------------------------------|-------------------|--------------------|-----------------------|--|--|
| U content, µg/kg | | | | | |
| Red siltstones 1 | 15.8±2.1 | 7±1 | 133±19 | 35±5 | 4319±447 |
| Red siltstones 2 | 30.5±3.9 | 19.8±2.5 | 52.7±7.2 | 159±21 | 1648±210 |
| Variegated siltstones | 30.9±4.1 | 109±15 | 90±11 | 873±113 | 4738±469 |
| Green siltstones 1 | 106±14 | 751±89 | 1157±123 | 3072±309 | 13714±1097 |
| Green siltstones 2 | 364±43 | 1496±163 | 848±95 | 1249±131 | 4371±371 |
| U content, % | | | | | |
| Red siltstones 1 | 0.35 | 0.16 | 3 | 0.7 | 95.8 |
| Red siltstones 2 | 1.6 | 1 | 2.8 | 8.3 | 86.3 |
| Variegated siltstones | 0.53 | 1.87 | 1.54 | 14.96 | 81.1 |
| Green siltstones 1 | 0.56 | 4 | 6.15 | 16.3 | 72.9 |
| Green siltstones 2 | 4.37 | 18 | 10.2 | 15 | 52.5 |

265

266 ²³⁴U:²³⁸U activity ratio

267 Increased values of $^{234}\text{U}:^{238}\text{U}$ activity ratio were noted in the material of red siltstones dissolved
 268 in water and 0.5M HCl. That is, uranium isotopes with elevated values of $^{234}\text{U}:^{238}\text{U}$ activity ratio
 269 (greater than 1) were deposited from groundwater on sorbent material and with iron hydroxides.
 270 Reduced values of $^{234}\text{U}:^{238}\text{U}$ activity ratio (less than 1) are characteristic of the most difficultly soluble
 271 fractions. In them, the dissolution of uranium by groundwater was practically absent and only
 272 depletion of ^{234}U atoms occurred due to recoil loss factor. In green siltstones, there is also a tendency
 273 towards a decrease in $^{234}\text{U}:^{238}\text{U}$ activity ratio in the direction from easily soluble fractions to sparingly
 274 soluble fractions (Fig. 3, interval 99.5–99.6 m). However, for a sample taken from the interval 66.7 -
 275 66.8 m, high values of $^{234}\text{U}:^{238}\text{U}$ activity ratio are observed in all mineral phases. Additional studies
 276 are needed to explain this fact.

277 *Evolution of uranium isotopic compositions*

278 The results obtained partially confirm previously expressed ideas about the evolution of U
 279 isotopic compositions of the Vendian rock near the study area [20]. It has been established that the
 280 processes of chemical weathering of Vendian deposits led to the formation of a strong oxidation
 281 zone, developed above 250 m.b.s.l. The inverse correlation between the concentrations of U and Fe
 282 (see Tables 1 and 2) in the red siltstones (increased Fe concentrations and reduced U contents) is a
 283 result of removal of U in oxidizing conditions, and accumulation of Fe. In red siltstones, the
 284 concentration of Fe_2O_3 is 5.3%, and the content of U is 1.9-4.5 mg/kg, in green siltstones the
 285 concentration of Fe_2O_3 is 2%, and the content of U is 5.8-18.8 mg/kg. Almost all U in the red siltstones
 286 has been replaced by a newly formed "hydrogenic" U (precipitated from groundwater), with an
 287 initial $^{234}\text{U}:^{238}\text{U}$ activity ratio \approx activity ratio of modern fresh groundwater = 3. The ending of the
 288 period of co-precipitation of hydrogenic uranium with iron hydroxide was estimated as 0.9 Ma,
 289 which should roughly correspond to the period of a sharp cold snap in the region. After, dissolution
 290 and desorption of hydrogenic U occurred during periods with no glaciations and marine
 291 transgressions.

292 Our results are consistent with the experimental results of Lowson et al. [16], Payne et al. [17],
 293 and Dabous et al. [18], which note the similarity of the $^{234}\text{U}:^{238}\text{U}$ activity ratios in groundwater and in
 294 the most easily leached fractions of water-bearing rocks.

295 At the same time, the lower average value of $^{234}\text{U}:^{238}\text{U}$ activity ratio 0.92 [20] was established in
 296 the samples of green siltstones taken in the paleovalley, which was screened by the layer of sea clays.
 297 It is explainable by the fact that these deposits have reached a steady state of the $^{234}\text{U}:^{238}\text{U}$ activity
 298 ratio that depends only on their size (the average grain size $\approx 30 \mu\text{m}$), because they were under
 299 reducing conditions over 1 Ma. A significantly higher content of uranium in them compared to red
 300 siltstones shows a considerable variability in the permeability values of the aquifer, whereby they
 301 were away from the paths of groundwater filtration and have retained uranium. The green siltstones
 302 studied in this work occur in the oxidative conditions of the aquifer which contains young fresh
 303 water [28]. They have high concentrations of uranium in readily soluble fractions and high $^{234}\text{U}:^{238}\text{U}$
 304 activity ratios. This can be explained by their deep processing by groundwater in a relatively recent
 305 period (tens - the first hundreds of thousands of years). During this processing, they were in a loose
 306 state, as a result of which U was evenly precipitated from water on the surface of disintegrated rock
 307 particles in the entire volume of the current green siltstones. Then there was cementation of rocks
 308 with Fe hydroxides, carbonates and clay material. After this, the rocks were again compacted under
 309 glacial loading. As the second option, it can be assumed that the green siltstones replace lenticular
 310 accumulations of organic matter with a high content of U adsorbed from groundwater. The place
 311 where 5 samples were taken for this study was the sea shelf of the Mikulinian (Eemian) Sea 115-130
 312 ka ago. Marine sediments up to 50-70 m thick contained a large amount (up to 10%) of organic
 313 residues of iodine-containing algae. Organic matter could enter sediments of the upper part of the
 314 Vendian Formation during the diagenesis of marine precipitation [42].

315 *Retardation factor*

316 Retardation factor is determined by the formula [43, 6]:

$$317 \quad R = 1 + M_s \cdot C_8^A / C_8^W \quad (2)$$

318 where $M_s = \rho_m(1-n) / \rho_{water}n$; C_8^A - solute concentration of ^{238}U in the stationary solid,
 319 $\mu\text{g}/\text{kg}$ [44]; C_8^W - measured concentration of ^{238}U in solution at the point of sampling, $\mu\text{g}/\text{kg}$; ρ_m -
 320 mineral density, g/cm^3 ; ρ_w - pore fluid density, g/cm^3 ; n - porosity.

321 For the study area, the following values of the parameters included in Eq. (2) were previously
 322 obtained: $C_8^W = 5 \mu\text{g/kg}$ (from 23 definitions of uranium concentrations in fresh water in a Vendian
 323 aquifer [28]; $n = 0.23$ (from 52 determinations) and $\rho_m = 2.75 \text{ g/cm}^3$ (from 52 determinations); $M_s =$
 324 9.2065 [27].

325 C_8^A can be taken as the average value of U content in adsorbed elements of the red siltstones =
 326 $23 \mu\text{g/kg}$ (Table 3), because green siltstones occupy an insignificant volume in the deposits of the
 327 Padun formation of the Vendian compared to red siltstones. However, this value characterizes the
 328 entire volume of rock that was crushed before the experiments. Under natural conditions, the
 329 movement of water in siltstones and sandstones occurs along pores and cracks, characterized by the
 330 value of open porosity. From this open volume, uranium adsorption occurs, which determines the
 331 value of the retardation factor. Therefore, as a first approximation, we can take:

$$332 \quad R = 1 + M_s \cdot C_8^A / C_8^W \cdot n \quad (3)$$

333 Calculations by the formula (3) give the value of the retardation factor 10.73.

334 In Malov [27], the average value of the ratio $R:p = 24$ was determined for a Vendian aquifer,
 335 where p is the recoil loss factor. That is, at $R = 10.73$, the value of p will be 0.45.

336 The obtained values (10.73 and 0.45) apparently characterize the upper limits of R and p ,
 337 respectively.

338 6. Conclusions

339 The partial extraction procedure was used to reconstruct the redistribution processes of
 340 uranium isotopes in certain mineral phases of the aquifer of sandy-clay deposits of the Vendian.

341 Red siltstones are depleted in uranium in relatively readily soluble mineral phases. The
 342 concentration of adsorbed uranium was established as $15.8 \pm 2.1 - 30.5 \pm 3.9 \mu\text{g/kg}$. This accounts for
 343 0.35 - 1.6% of its total amount in rocks of this type. Carbonate minerals contain even less uranium:
 344 $7 \pm 1 - 19.8 \pm 2.5 \mu\text{g/kg}$, i.e. 0.16 - 1%. In iron hydroxides and the most readily soluble aluminosilicates,
 345 uranium concentrations are in the range $168 \pm 24 - 212 \pm 28 \mu\text{g/kg}$. The most insoluble fraction contains
 346 $1.65 \pm 0.21 - 4.32 \pm 0.45 \text{ mg/kg}$ of uranium. In green siltstones, the concentration of adsorbed uranium
 347 is much higher: $106 \pm 14 - 364 \pm 43 \mu\text{g/kg}$ (0.56 - 4.37%). Carbonate minerals and amorphous iron oxides
 348 contain $1.91 \pm 0.21 - 2.34 \pm 0.26 \text{ mg/kg}$ of uranium. In aluminosilicates and a clay/quartz resistate,
 349 uranium concentrations are $5.6 \pm 0.5 - 16.8 \pm 1.4 \text{ mg/kg}$. Such a distribution of uranium in various types
 350 of rocks is consistent with the earlier assumption about the removal of uranium from red siltstones
 351 in the last 0.9 Ma and its conservation in green siltstones.

352 Elevated values of $^{234}\text{U}:^{238}\text{U}$ activity ratio prevail in the adsorbed material and iron hydroxides.
 353 In aluminosilicates and clay/quartz resistate, the values decrease. This indicates the replacement of
 354 primary sedimentogenic uranium by secondary hydrogenic uranium adsorbed on the surface of
 355 minerals and coprecipitated with iron hydroxides.

356 The results obtained made it possible to carry out preliminary quantitative estimates of the
 357 retardation factor and recoil loss factor of uranium in the groundwater of siltstones of the Vendian
 358 aquifer.

359 At the same time, some uncertainty in the interpretation of the high U contents and high
 360 $^{234}\text{U}:^{238}\text{U}$ activity ratios in green siltstones obtained in this work should be noted. This requires
 361 additional research on a more representative number of samples. Also, the relationship between the
 362 extraction solutions and the mineral phases has not yet been precisely established. The mineral
 363 phases that were dissolved during the sequential extraction procedure should be examined using
 364 X-ray powder diffraction (XRD) analysis and scanning electron microscopy (SEM).

365 **Acknowledgments:** This work was supported by the Russian Ministry of Education and Science
 366 (project no. № AAAA-A19-119011890018-3), the UB RAS (project no. AAAA-A18-118012390242-5),
 367 the Russian Foundation for Basic Research (projects no. 20-05-00045_A, 18-05-60151_Arctic; no.
 368 18-05-01041_A). The authors are grateful to T.N. Markova for the description of the samples of the
 369 studied rocks was performed on five thin sections of core samples.

370 **Conflicts of Interest:** The authors declare no conflict of interest. The founding sponsors had no role
371 in the design of the study; in the collection, analyses, or interpretation of data; in the writing of the
372 manuscript, and in the decision to publish the results.

373 **Author Contributions:** Conceptualization, formal analysis, writing—original draft preparation,
374 Alexander I. Malov; methodology and investigation, Sergey B. Zykov.

375 Appendix A

376 Description of the thin sections of core samples

377 Thin sections of core samples (n=5) were prepared in epoxy resin. Thin sections were
378 examined under transmitted, polarized, and reflected light using optical microscopy to determine
379 the minerals and the textural features of the rocks.

380 1. *Green siltstones 66.7-66.8 m*

381 The sandy siltstone has a light greenish-gray color. The texture of the rock is heterogeneous,
382 due to the chaotic arrangement of clastic grains and the presence of spots up to 0.4 mm in size with
383 an iron-carbonate aggregate. Clastic material is 70-80% and is represented by grains of quartz,
384 feldspar and quartzite rocks; the composition is dominated by quartz grains. Among feldspars
385 where plagioclases and potassium feldspars are diagnosed, plagioclases prevail. The grain size
386 varies from 0.02 to 0.15 mm; grains up to 0.2 mm in size are rarely found. The surface of the grains is
387 corrosive. Single grains of accessory minerals are noted - tourmaline, ilmenite, epidote, zircon. On
388 separate grains of quartz and feldspar, a regenerative rim is fixed. Some fragments of quartz and
389 feldspar are sericitized. In the rock, single plates of colorless and colored mica up to 0.15-0.25 mm
390 in size are diagnosed; this mica is diagenetic. Film-pore clay-ferruginous cement predominates, and
391 cementation due to regeneration is also fixed. Marks, lenses (not exceeding 0.4-0.5 mm in size) with
392 limonite-goethite and ferruginous-carbonate cement are noted. Carbonate is represented by calcite
393 and it is formed later than limonite-goethite aggregate. Individual detrital grains are partially
394 replaced by a ferruginous carbonate aggregate. Limonite-goethite and carbonate aggregates in
395 cement are epigenetic. Most likely, compaction of sedimentary material, hydromica of cement in
396 siltstone, and a high content of deformed plates are associated with dynamic changes. That is, the
397 structural adjustment of cement is due to the influence of tectonic processes and hydrothermal
398 solutions in the process of formation of kimberlite fields.

399 2. *Red sandstones 75.2-75.3 m*

400 Sandstone oligomictic fine-grained silty has brown color with light streaks. Rounded spots
401 1.0–2.0 mm in size with carbonate cement are fixed in the rock; their location is subparallel. The
402 slanting texture due to particle size distribution is not clearly expressed. In some areas, a random
403 distribution of clastic material is noted. Clastic material is represented by grains of quartz, feldspar
404 and quartzite rocks; the composition is dominated by quartz grains. The size of clastic grains varies
405 from 0.03-0.04 mm to 0.2-0.25 mm. Grain rounding is mostly good and medium. The grain surface is
406 corrosive; regenerative rim is fixed on separate fragments of quartz and feldspar. Separate
407 fragments of quartz and feldspar are sericitized. There are single plates of green mica up to 0.12-0.15
408 mm in size, which fill individual pores and sometimes partially replace detrital grains. Most likely
409 this mica is epigenetic. Film-pore clay-ferruginous cement predominates, and cementation due to
410 regeneration is also fixed. Spots with limonite-goethite and ferruginous-carbonate cement are noted.
411 Carbonate is represented by calcite and is formed later than limonite-goethite aggregate. Individual
412 detrital grains are partially replaced by a ferruginous carbonate aggregate. Limonite-goethite and
413 carbonate aggregates in cement are epigenetic.

414 3. *Variiegated siltstones 83.9-84 m*

415 Siltstone with indistinctly expressed oblique and banded textures. Striping does not coincide
416 with layering; alternation of brown and gray, greenish-gray rocks does not form layers.
417 Cross-bedding is due to the presence of argillite microlenses. The composition of this rock does not
418 differ from the sandstones and siltstones that are described in the above.

419 4. *Red siltstones 94-94.1 m*

420 Oligomictic siltstone of brown color with indistinctly expressed cross-layered texture. The
421 oblique texture is due to a poorly defined granulometric sorting of clastic material and the presence

422 of argillite microlenses. Breccia is due to the presence of areas with a random distribution of clastic
 423 material, which is associated with sedimentation processes. The presence of sites with
 424 limonite-goethite cement is due to epigenetic processes. Clastic material, as in previous thin sections,
 425 is represented by grains of quartz, feldspar and quartzite rocks, quartz grains dominate in the
 426 composition. The size of clastic grains varies from 0.03-0.04 mm to 0.15-0.2 mm. Grain rounding is
 427 mostly average and good. The grain surface is corrosive; a regenerative rim is fixed on separate
 428 fragments of quartz and feldspar. Some fragments of quartz and feldspar are sericitized. Rare plates
 429 of colorless mica, which are diagenetic, are fixed in this strain. By the nature of the filling, the
 430 cement is not continuous, the number of hollow pores is insignificant. Film-pore clay-ferruginous
 431 cement predominates, and cementation due to regeneration is also fixed. Spots with
 432 limonite-goethite and ferruginous-carbonate cement are noted. Carbonate is represented by calcite
 433 and it is later than limonite-goethite aggregate. Limonite-goethite and carbonate aggregates in
 434 cement are epigenetic.

435 5. *Green siltstones 99.5-99.6 m*

436 Oligomictic siltstone sandy with indistinctly expressed oblique and banded textures. The
 437 color of the strain is light greenish gray. In terms of composition and structural-textural features,
 438 siltstone does not differ from the rocks that are described in the above.

439 References

- 440 1. Chkir, N., Guendouz, A., Zouari, K., Hadj Ammar, F., Moulla, A.S.. Uranium isotopes in groundwater
 441 from the continental intercalaire aquifer in Algerian Tunisian Sahara (northern Africa). *J. Environ. Radioact.*
 442 **2009**, *100*, 649–656.
- 443 2. Dhaoui, Z., Chkir, N., Zouari, K., Ammar, F.H., Agoune, A. Investigation of uranium geochemistry along
 444 groundwater flow path in the Continental Intercalaire aquifer (Southern Tunisia). *J. Environ. Radioact.*
 445 **2016**, *157*, 67–76.
- 446 3. Priestley, S.C., Payne, T.E., Harrison, J.J., Post, V.E.A., Shand, P., Love, A.J., Wohling, D.L. Use of
 447 U-isotopes in exploring groundwater flow and inter-aquifer leakage in the south-western margin of the
 448 Great Artesian Basin and Arckaringa Basin, central Australia. *Appl. Geochem.* **2018**, *98*, 331–344.
- 449 4. Suksi, J., Rasilainen, K., Marcos, N. U isotopic fractionation - a process characterising groundwater
 450 systems. In: Merkel, B.J., Hasche-Berger, A. (eds), *Uranium in the Environment*. Springer-Verlag: Berlin,
 451 Heidelberg, **2006**; pp. 683-690.
- 452 5. Chabaux, F., Bourdon, B., Riotte, J. U-series geochemistry in weathering profiles, riverwaters and lakes. In:
 453 Krishnaswami, S., Cochran, J.K. (eds), *U/Th series radionuclides in aquatic systems*, vol 13, Radioactivity in
 454 the environment. Elsevier: New York, **2008**; pp. 49–104.
- 455 6. Porcelli, D. Investigating groundwater processes using U- and Th-series nuclides. *Radioact. Environ.* **2008**,
 456 *13*, 105–153.
- 457 7. Maher, K., DePaolo, D.J., Lin, J.C.F. Rates of silicate dissolution in deep-sea sediment: in situ measurement
 458 using U-234/U-238 of pore fluids. *Geochim. Cosmochim. Acta* **2004**, *68*, 4629-4648.
- 459 8. Ivanovich, M., Fröhlich, K., Hendry, M.J. Uranium-series radio nuclides in fluids and solids, Milk River
 460 aquifer, Alberta, Canada. *Appl. Geochem.* **1991**, *6*, 405–418.
- 461 9. Chabaux, F., Dequincey, O., Leveque, J.J., Leprun, J.C., Clauer, N., Riotte, J., Paquet, H. Tracing and
 462 dating recent chemical transfers in weathering profiles by trace-element geochemistry and
 463 U-238-U-234-Th-230 disequilibria: the example of the Kaya lateritic toposequence (Burkina-Faso). *CR*
 464 *Geosci* **2003**, *335*, 1219–1231.
- 465 10. Dosseto, A., Bourdon, B., Turner, S. Uranium-series isotopes in river materials: Insights into the
 466 timescales of erosion and sediment transport. *Earth Planet Sci Lett* **2008**, *265*, 1–17.

- 467 11. Vigier, N., Bourdon, B. Chapter 27. Constraining Rates of Chemical and Physical Erosion Using U-Series
468 Radionuclides. In: M. Baskaran (ed.), *Handbook of Environmental Isotope Geochemistry, Advances in Isotope*
469 *Geochemistry*. Springer-Verlag: Berlin, Heidelberg, **2011**, pp. 553-571.
- 470 12. Duff, M.C., Coughlin, J.U., Hunter, D.B. Uranium co-precipitation with iron oxide minerals. *Geochim*
471 *Cosmochim Acta* **2002**, *66*, 3533–3547.
- 472 13. Giammar, D.E., Hering, J.G. Timescale for sorption-desorption and surface precipitation of uranyl on
473 goethite. *Environ Sci Technol* **2001**, *35*, 3332–3337.
- 474 14. Singer, D.M., Maher, K., Brown, G.E. Jr. Uranyl-chlorite sorption/desorption: evaluation of different U(VI)
475 sequestration processes. *Geochim Cosmochim Acta* **2009**, *73*, 5989–6007.
- 476 15. Tricca, A., Wasserburg, G. J., Porcelli, D., Baskaran, M. The transport of U- and Th-series nuclides in a
477 sandy unconfined aquifer. *Geochim. Cosmochim. Acta* **2001**, *65*, 1187–1210.
- 478 16. Lowson, R.T., Short, S.A., Davey, B.G., Gray, D.J. $^{234}\text{U}/^{238}\text{U}$ and $^{230}\text{Th}/^{234}\text{U}$ activity ratios in mineral phases
479 of a lateritic weathered zone. *Geochim. Cosmochim. Acta* **1986**, *50*, 1697–1702.
- 480 17. Payne, T.E., Edis, R., Fenton, B.R., Waite, T.D. Comparison of laboratory uranium sorption data with 'in
481 situ distribution coefficients' at the Koongarra uranium deposit, Northern Australia. *J. Environ. Radioact.*
482 **2001**, *57*, 35–55.
- 483 18. Dabous, A.A., Osmond, J.K., Dawood, Y.H. Uranium/thorium isotope evidence for groundwater history
484 in the Eastern Desert of Egypt. *J. Arid Environ.* **2002**, *50*, 343–357.
- 485 19. Yanase, N., Nightingale, T., Payne, T., Duerden, P. Uranium distribution in mineral phases of rock by
486 sequential extraction procedure. *Radiochim. Acta* **1991**, 52-53, 387-393.
- 487 20. Malov, A.I. Evolution of the uranium isotopic compositions of the groundwater and rock in the
488 sandy-clayey aquifer. *Water (Switzerland)* **2017**, *9* (12), 910.
- 489 21. DePaolo, D.J., Maher, K., Christensen, J.N., McManus, J.,. Sediment transport time measured with
490 U-series isotopes: Results from ODP North Atlantic drift site 984. *Earth Planet Sci Lett* **2006**, *248*, 394–410.
- 491 22. Maher, K., DePaolo, D.J., Christensen, J.N. U-Sr isotopic speedometer: fluid flow and chemical weathering
492 rates in aquifers. *Geochim Cosmochim Acta* **2006**, *70*, 4417–4435.
- 493 23. Tessier, A., Campbell, P.G.C., Bisson, M. Sequential extraction procedure for the speciation of particulate
494 trace metals. *Anal. Chem.* **1979**, *51*, 848–851.
- 495 24. Hall, G.E.M., Vaive, J.E., Beer, R., Hoashi, M. Selective leaches revisited, with emphasis on the
496 amorphous Fe oxyhydroxide phase extraction. *J. Geochem. Explor.* **1996**, *56*, 59–78.
- 497 25. Quevauviller Ph., Rauret, G., López-Sánchez, J.-F., Rubio, R., Ure, A., Muntau, H. Certification of trace
498 metal extractable contents in a sediment reference material (CRM601) following a three-step sequential
499 extraction procedure. *Sci. Total Environ.* **1997**, *205*, 223–234.
- 500 26. Sutherland, R.A., Tack, F.M.G., Tolosa, C.A., Verloo, M.G. Metal Extraction from Road Sediment using
501 Different Strength Reagents: Impact on Anthropogenic Contaminant Signals. *Environ Monit Assess* **2001**,
502 *71*-3, 221-242. <https://doi.org/10.1023/A:1011810319015>
- 503 27. Malov, A.I. Estimation of uranium migration parameters in sandstone aquifers. *J. Environ. Radioact.* **2016**,
504 *153*, 61-67.
- 505 28. Malov, A.I. Evolution of the groundwater chemistry in the coastal aquifers of the south-eastern White Sea
506 area (NW Russia) using ^{14}C and ^{234}U - ^{238}U dating. *Sci. Total Environ.* **2018**, [616–617](#), 1208-1223.
- 507 29. Andreas, J.N., and Kay, R.L.F. The evolution of enhanced $^{234}\text{U}/^{238}\text{U}$ activity ratios for dissolved uranium
508 and groundwater dating. 4th Int. Conf. on Geochronology, Cosmochronology and Isotope Geology,
509 Denver, Colo., 1978. *U.S. Geol. Surv., Open-File Rep.* **1978**, 78-701, 11-13.

- 510 30. Fröhlich, K., and Gellermann, R. On the potential use of uranium isotopes for groundwater dating. *Chem.*
511 *Geol.* **1987**, *65*, 67-77.
- 512 31. Andreas, J.N., and Kay, R.L.F. The U content and $^{234}\text{U}/^{238}\text{U}$ activity ratios of dissolved uranium in
513 groundwaters from Triassic sandstones in England. *Isotope Geoscience* **1983**, *1*, 101- 117.
- 514 32. Stankovsky, A.F., Verichev, E.M., Grib, V.P., et al. The Vendian in the Southeastern White Sea Region. *Izv.*
515 *Akad. Nauk SSSR, Ser. Geol.* **1981**, *2*, 78–87.
- 516 33. Stankovsky, A.F., Verichev, E.M., Dobeiko, I.P. The Vendian in Southeastern White Sea Region. In: *The*
517 *Vendian: Historical-Geological and Paleontological Evidence*, vol. 2: Stratigraphy and Geological Processes.
518 Nauka: Moscow, **1985**, 67–76 (in Russian).
- 519 34. Malov, A.I. Water-Rock Interaction in Vendian Sandy-Clayey Rocks of the Mezen Syncline. *Lithol. Miner.*
520 *Resour.* **2004**, *39-4*, 345–356.
- 521 35. Grazhdankin, D.V., Podkovyrov, V.N., Maslov, A.V. Paleoclimatic Environments of the Formation of
522 Upper Vendian Rocks on the Belomorian-Kuloi Plateau, Southeastern White Sea Region. *Lithol Miner*
523 *Resour* **2005**, *40*, 232. <https://doi.org/10.1007/s10987-005-0024-x>
- 524 36. Bonotto, D.M., Andrews, J.N. The mechanism of $^{234}\text{U}/^{238}\text{U}$ activity ratio enhancement in karstic limestone
525 groundwater. *Chem. Geol. (Isot. Geosci. Sec.)* **1993**, *103*, 193-206.
- 526 37. Bonotto, D.M., Andrews, J.N. The transfer of uranium isotopes ^{234}U and ^{238}U to the waters interacting
527 with carbonates from Mendip Hills area (England). *Appl. Radiat. Isotopes* **2000**, *52*, 965-983.
- 528 38. Singh, S. P., Tack, F. M. G., Verloo, M. G. Solid-phase distribution of heavy metals as affected by single
529 reagent extraction in dredged sediment derived surface soils. *Chem. Spec. Bioavail.* **1996**, *8*, 37–43.
- 530 39. Malyshev, V.I., Bakhur, A.E., Manuylova, L.I. et al. *Methods for measuring the volumetric activity of uranium*
531 *isotopes (234 , 238) in natural water sample alpha spectrometry with radiochemical separation*. VIMS: Moscow,
532 **1999a** (in Russian).
- 533 40. Fröhlich, K. Dating of old groundwater using uranium isotopes – principles and applications. In: *Isotope*
534 *methods for dating old groundwater*. IAEA: Vienna, **2013**, 153-178.
- 535 41. Malyshev, V.I., Bakhur, A.E., Manuylova, L.I. et al. Methods for measuring the specific activity of
536 uranium isotopes (234 , 238) in soils, sediments, rocks and building materials alpha spectrometry with
537 radiochemical separation. VIMS: Moscow, **1999b** (in Russian).
- 538 42. Malov, A.I. Application of Geological Benchmarks for Determining Groundwater Residence Time in the
539 Aquifer Based on Uranium Isotope Data: Evidence from the Severnaya Dvina Basin. *Lithol. Miner. Resour.*
540 **2013**, *48-3*, 254–265.
- 541 43. Krishnaswami, S., Graustein, W. C., Turekian, K. K., and Dowd, J. F. Radium, thorium and radioactive
542 lead isotopes in groundwaters: Application to the in situ determination of adsorption-desorption rate
543 constants and retardation factors. *Water Resources Res.* **1982**, *18*, 1663-1675.
- 544 44. Pearson, F.J., Norowha, C.J., Andrews, R.W. Mathematical modelling of the distribution of natural ^{14}C ,
545 ^{234}U , and ^{238}U in a regional groundwater system, *Radiocarbon* **1983**, *25*, 291–300.